

Large- $N$  phase transition in lattice 2-d principal chiral models.

Massimo Campostrini, Paolo Rossi, and Ettore Vicari

*Dipartimento di Fisica dell'Università and I.N.F.N., I-56126 Pisa, Italy*

We investigate the large- $N$  critical behavior of 2-d lattice chiral models by Monte Carlo simulations of  $U(N)$  and  $SU(N)$  groups at large  $N$ . Numerical results confirm strong coupling analyses, i.e. the existence of a large- $N$  second order phase transition at a finite  $\beta_c$ .

11.15.Me, 11.10.Kk, 11.15.Pg

arXiv:hep-lat/9412102v1 24 Dec 1994

## I. INTRODUCTION

Strong coupling studies of lattice 2-d principal chiral models, with the standard nearest-neighbour interaction

$$S_L = -2N\beta \sum_{x,\mu} \text{ReTr} \left[ U(x) U^\dagger(x+\mu) \right] , \quad \beta = \frac{1}{NT} , \quad (1)$$

have shown evidence of a large- $N$  phase transition at a finite  $\beta_c$ , separating the strong coupling and the weak coupling regions [1,2]. An analysis of the 18<sup>th</sup> order  $N = \infty$  strong coupling series of the specific heat showed a second order critical behavior

$$C \sim |\beta - \beta_c|^{-\alpha} , \quad (2)$$

with the following estimates of  $\beta_c$  and  $\alpha$ :  $\beta_c = 0.3058(3)$  and  $\alpha = 0.23(3)$  [2,3]. This critical phenomenon is somehow effectively decoupled from the continuum limit ( $\beta \rightarrow \infty$ ), indeed dimensionless ratios of physical quantities are reproduced with great accuracy even for  $\beta < \beta_c$  [4,2].

A critical behavior at  $N = \infty$  is also present in 1-d lattice chiral models, where at  $N = \infty$  the free energy is piecewise analytical with a third order transition between the strong coupling and weak coupling domains [5]. In these models the parameter  $N$  plays a role analogous to the volume in ordinary systems with a finite number of degrees of freedom per site, and the double scaling limit describing the simultaneous approach  $N \rightarrow \infty$  and  $\beta \rightarrow \beta_c$  is shown to be equivalent to finite size scaling of 2-d spin systems close to the criticality [6,7].

In this paper we investigate the above large- $N$  critical phenomenon by Monte Carlo simulations, that is by extrapolating, possibly in a controlled manner, numerical results at sufficiently large  $N$ , in the same spirit of the double scaling limit technique developed in the studies of 1-d matrix models. We performed Monte Carlo simulations of  $SU(N)$  and  $U(N)$  models for several large values of  $N$ , studying the approach to  $N = \infty$ . Some  $SU(N)$  Monte Carlo results at large  $N$  were already presented in Ref. [4]. Since  $SU(N)$  and  $U(N)$  models are expected to have the same large- $N$  limit,  $U(N)$  Monte Carlo results provide further information and check of the  $N \rightarrow \infty$  behavior of lattice principal chiral models.

In the continuum limit  $SU(N)$  and  $U(N)$  2-d lattice actions should describe the same theory even at finite  $N$ , in that the additional  $U(1)$  degrees of freedom of the  $U(N)$  models decouple. The  $U(N)$  lattice action, when restricting ourselves to its  $SU(N)$  degrees of freedom, represents a different regularization of the  $SU(N) \times SU(N)$  chiral field theory. One loop calculations in perturbation theory give the following  $\Lambda$ -parameter ratios

$$\frac{\Lambda_{MS}^U}{\Lambda_L^U} = \sqrt{32} \exp\left(\frac{\pi}{2}\right) , \quad (3)$$

$$\frac{\Lambda_L^{SU}}{\Lambda_L^U} = \exp\left(\frac{\pi}{N^2}\right) , \quad (4)$$

where  $\Lambda_L^U$  and  $\Lambda_L^{SU}$  are respectively the  $\Lambda$ -parameters of the  $U(N)$  and  $SU(N)$  lattice actions (1).

The fundamental group invariant correlation function of  $SU(N)$  models is

$$G(x) = \frac{1}{N} \langle \text{Tr} [U^\dagger(x)U(0)] \rangle . \quad (5)$$

Introducing its lattice momentum transform  $\tilde{G}(p)$ , we define the magnetic susceptibility  $\chi = \tilde{G}(0)$ , and the second moment correlation length

$$\xi_G^2 = \frac{1}{4 \sin^2 \pi/L} \left[ \frac{\tilde{G}(0,0)}{\tilde{G}(0,1)} - 1 \right] . \quad (6)$$

In the  $U(N)$  case we consider two Green's functions. One describes the propagation of  $SU(N)$  degrees of freedom:

$$G(x) = \frac{1}{N} \langle \text{Tr} [\hat{U}^\dagger(x)\hat{U}(0)] \rangle ,$$

$$\hat{U}(x) \equiv \frac{U(x)}{(\det U(x))^{1/N}} . \quad (7)$$

The other describes the propagation of the  $U(1)$  degrees of freedom associated with the determinant of  $U(x)$ :

$$G_d(x) = \langle (\det [U^\dagger(x)U(0)])^{1/N} \rangle , \quad (8)$$

From the Green's functions  $G(x)$  and  $G_d(x)$  we can define the corresponding magnetic susceptibilities  $\chi$ ,  $\chi_d$  and second moment correlation lengths  $\xi_G$ ,  $\xi_d$ .

At finite  $N$ , while  $SU(N)$  lattice models do not have any singularity at finite  $\beta$ ,  $U(N)$  lattice models should undergo a phase transition, driven by the  $U(1)$  degrees of freedom corresponding to the determinant of  $U(x)$ , and following a pattern similar to the 2-d XY model [8]. The mass propagating in the determinant channel  $M_d$  should vanish at a finite value  $\beta_d$  and stay zero for larger  $\beta$ . Then for  $\beta > \beta_d$  this sector of the theory decouples from the other ( $SU(N)$ ) degrees of freedom, which are those determining the continuum limit of principal chiral models for  $\beta \rightarrow \infty$ . We recall that the 2-d XY model critical behavior is characterized by a sharp approach to the critical point  $\beta_{XY}$  ( the correlation length grows exponentially), a line of fixed point for  $\beta > \beta_{XY}$ , and a finite specific heat having a peak for a  $\beta < \beta_{XY}$  (see e.g. Ref. [9]).

## II. NUMERICAL RESULTS.

### A. The Monte Carlo algorithm.

In our simulations we used local algorithms containing overrelaxation procedures. In the  $SU(N)$  case, we employed the Cabibbo-Marinari algorithm [10] to upgrade  $SU(N)$  matrices by updating their  $SU(2)$  subgroups, chosen randomly among the  $\frac{N(N-1)}{2}$  subgroups acting on each  $2 \times 2$  submatrix. At each site the  $SU(2)$  subgroup identified by the indices  $i, j$  ( $1 \leq i < j \leq N$ ) was updated with a probability  $P = \frac{2}{N-1}p$ , so that the average number

of  $SU(2)$  updatings per  $SU(N)$  site variable was  $\bar{n} = pN$ . In our simulations we always chose  $p \lesssim 1$ , decreasing  $p$  when increasing  $N$ . We used  $p \simeq 1$  at  $N = 9$ ,  $p \simeq 2/3$  at  $N = 15$  and  $p \simeq 1/2$  at  $N = 21, 30$ . The extension to the  $U(N)$  case is easily achieved by updating, beside  $SU(2)$  subgroups,  $U(1)$  subgroups. In our simulations we upgraded the  $U(1)$  subgroups identified by the diagonal elements of the  $U(N)$  matrix. The  $SU(2)$  and  $U(1)$  updatings were performed by a mixture of over-heat-bath algorithm [11] (90%) and standard heat-bath (10%). At fixed parameter  $p$ , the number of operations per site increases as  $N^2$  at large  $N$ .

The above algorithm experiences a critical slowing down in  $N$ , that is keeping the correlation length fixed the autocorrelation time grows with increasing  $N$ . This effect is partially compensated by a reduction of the fluctuations of group invariant quantities when  $N$  grows. In the  $U(N)$  simulations the quantities related to the determinant channel are subjected to large fluctuations, causing large errors in the measurements.

In Tables I and II we present Monte Carlo data respectively for the  $U(N)$  and  $SU(N)$  simulations. Finite size systematic errors in evaluating infinite volume quantities should be smaller than the statistical errors of all numerical results presented in this paper.

## B. Numerical evidence of a large- $N$ phase transition.

Lattice chiral models have a peak in the specific heat

$$C = \frac{1}{N} \frac{dE}{dT} \quad (9)$$

which becomes sharper and sharper with increasing  $N$ . In Figs. 1 and 2 we plot the specific heat respectively for the  $U(N)$  and  $SU(N)$  models. Such a behavior of the specific heat should be an indication of a phase transition for  $N = \infty$  at a finite  $\beta_c$ . The positions of the peaks  $\beta_{peak}$  in  $SU(N)$  and  $U(N)$  converge from opposite directions, restricting the possible values of  $\beta_c$  to  $0.304 \lesssim \beta_c \lesssim 0.309$ . Notice that Monte Carlo data for  $\beta \lesssim \beta_c \simeq 0.306$  approach, for growing  $N$ , the resummed 18<sup>th</sup> order large- $N$  strong coupling series of the specific heat [3]; in this region, as expected by strong coupling considerations, the convergence of  $U(N)$  models is faster.

A more accurate estimate of the critical coupling  $\beta_c$  can be obtained by using a finite  $N$  scaling Ansatz

$$\beta_{peak}(N) \simeq \beta_c + cN^{-\epsilon}, \quad (10)$$

in order to extrapolate  $\beta_{peak}(N)$  to  $N \rightarrow \infty$ . The above Ansatz is suggested by the idea that the parameter  $N$  may play a role quite analogous to the volume in the ordinary systems close to the criticality. This idea was already exploited in the study of 1-d matrix models [12,6,7], where double scaling limit turned out to be very similar to finite size scaling in a two-dimensional critical phenomenon. Substituting  $L \rightarrow N$  and  $1/\nu \rightarrow \epsilon$ , Eq. (10) becomes the well-known finite size scaling relationship derived in the context of the renormalization group theory. Furthermore the exponent  $\epsilon$  should be the same in the  $U(N)$  and  $SU(N)$  models, in that it should be a critical exponent associated to the  $N = \infty$  phase transition. Notice that the function  $\beta_{peak}(N)$  in Eq. (10) is considered at infinite space volume.

In the study of ordinary critical phenomena the reweighting technique [13], turns out to be very efficient to determine quantities like the position of the specific heat peak. In our work we could use this technique only for  $N = 9$ , since for larger  $N$  the reweighting range around the point where the simulation is performed turned out to be much smaller than the typical  $\beta$  interval of our simulations. For  $N \geq 15$   $\beta_{peak}(N)$  data and their errors were estimated from the specific heat data reported in the Tables I and II, supported by the direct measurements of the specific heat derivatives at each  $\beta$ .

Our estimates of  $\beta_{peak}$  at  $N = 9, 15, 21$  for  $U(N)$  and  $N = 9, 15, 21, 30$  for  $SU(N)$  fit very well formula (10). By a fit with four free parameters,  $\beta_c$ ,  $\epsilon$ ,  $c_{U(N)}$  and  $c_{SU(N)}$ , we found

$$\begin{aligned}\beta_c &= 0.3057(3), \\ \epsilon &= 1.45(8).\end{aligned}\tag{11}$$

In Fig. 3 the fit result is compared with the  $\beta_{peak}(N)$  data. A fit with two independent  $\epsilon$  exponents,  $\epsilon_{U(N)}$  and  $\epsilon_{SU(N)}$  gave compatible results, but larger errors. Notice that this Monte Carlo estimate of  $\beta_c$  is in agreement with the determination (2) coming from strong coupling computations.

We checked the finite  $N$  scaling Ansatz (10) in the similar context of the large- $N$  phase transition of 1-d lattice  $U(N)$  chiral models with free boundary conditions, where the critical point  $\beta_c$  and the critical exponents  $\nu$  and  $\alpha$  are known:  $\beta_c = 1/2$ ,  $\nu = 3/2$  and  $\alpha = -1$ . We computed the position of the specific heat peak at finite  $N$  finding the asymptotic behavior (10) with  $\epsilon = 2/3$ . Details on these calculations are given in the Appendix. As already mentioned, from standard finite size scaling arguments the critical exponent  $\epsilon$  should be related to the critical exponent  $\nu$ :  $\epsilon = 1/\nu$ . Notice that the critical exponents  $\nu$  and  $\alpha$  satisfy a two-dimensional hyperscaling relation:  $2\nu = 2 - \alpha$ . In 1-d lattice chiral models the number  $d_e = 2$  of effective dimensions of the large- $N$  critical phenomenon is related to the fact that the double limit  $N \rightarrow \infty$  and  $\beta \rightarrow \beta_c$  is equivalent to the continuous limit of a two-dimensional gravity model with central charge  $c = -2$ .

Since the large- $N$  phase transition of the 2-d lattice chiral models is of the second order type, its behavior cannot be found in the classification of double scaling limits of Refs. [14,5], which are parametrized by a central charge  $c < 1$  implying  $\alpha < 0$ . Moreover, unlike 1-d lattice chiral models, the interpretation of the large- $N$  phase transition of 2-d lattice chiral models as an effective  $d_e = 2$  ordinary critical phenomenon does not seem to be valid: in fact, if  $\epsilon = 1/\nu$ , by substituting our estimates of  $\alpha$  and  $\epsilon$  in the hyperscaling relation  $d_e = (2 - \alpha)\epsilon$  we would obtain  $d_e = 2.6(2)$ . A more general thermodynamic inequality would give  $d_e \geq (2 - \alpha)\epsilon$  [16].

Monte Carlo data of  $\chi$  and  $\xi_G$  for  $\beta \lesssim \beta_c$  compare very well with the large- $N$  strong coupling series of  $\chi$  (up to 15<sup>th</sup> order) and  $\xi_G$  (up to 14<sup>th</sup> order) [2]. Fig. 4, where  $\xi_G$  is plotted versus  $\beta$ , shows that data approach, with growing  $N$ , the curve obtained by resumming the strong coupling series of  $\xi_G$  [3], and in particular the  $U(N)$  data, whose convergence is faster, are in quantitative agreement.

Large- $N$  numerical results seem to indicate that all physical quantities, such as  $\chi$  and  $\xi_G$ , are well behaved functions of the internal energy  $E$  even at  $N = \infty$  [4]. Therefore as a consequence of the specific heat divergence at  $\beta_c$ , the  $N = \infty$   $\beta$ -function  $\beta_L(T) \equiv -adT/da$  should have a non-analytical zero at  $\beta_c$ , that is  $\beta_L(\beta) \sim |\beta - \beta_c|^\alpha$  in the neighbourhood of  $\beta_c$ .

By defining a new temperature proportional to the energy [17], this singularity disappears, and one can find good agreement between the measured mass scale and the asymptotic scaling predictions in the “energy” scheme even for  $\beta < \beta_c$ , where strong coupling expansion is expected to converge [4]. In fact strong coupling computations show asymptotic scaling with a surprising accuracy of few per cent [2].

In the  $U(N)$  case, a Kosterlitz-Thouless phase transition driven by the determinant is expected at  $\beta_d > \beta_{peak}$  for each finite  $N$ . Our data seem to support this picture, indeed after the peak of  $C$ , the magnetic susceptibility  $\chi_d$  and the second moment correlation length  $\xi_d$  defined from the determinant correlation function (8) begin to grow very fast. In Fig. 5 we plot  $\chi_d$  versus  $\beta$ . Green and Samuel argued (using strong coupling and weak coupling arguments) that the large- $N$  phase transition is nothing but the large- $N$  limit of the determinant phase transition present in the  $U(N)$  lattice models [8,18]. According to this conjecture, in the large- $N$  limit  $\beta_d$  and  $\beta_{peak}$  should both converge to  $\beta_c$ , and the order of the determinant phase transition would change from an infinite order of the Kosterlitz-Thouless mechanism to a second order with divergent specific heat. The large- $N$  phase transition of the  $SU(N)$  models could then be explained by the fact that the large- $N$  limit of the  $SU(N)$  theory should be the same as the large- $N$  limit of the  $U(N)$  theory. Our numerical results give only a partial confirm of this scenario, we can just hint from the behavior of  $\chi_d$  and  $\xi_d$  with growing  $N$  that the expected phase transition is moving toward  $\beta_c$ . The large- $N$  strong coupling series of the mass  $M_d$  propagating in the determinant channel has been calculated up to 6<sup>th</sup> order, indicating a critical point, determined by the zero of the  $M_d$  series, slightly larger than our determination of  $\beta_c$ :  $\beta_d(N = \infty) \simeq 0.324$  [8]. This discrepancy could be explained either by the shortness of the strong coupling series of  $M_d$ , or by the fact that such a determination of  $\beta_c$  relies on the absence of non-analyticity points before the strong coupling series of  $M_d$  vanishes, and therefore a non-analyticity at  $\beta_c \simeq 0.306$  would invalidate all strong coupling predictions for  $\beta > \beta_c$ .

### C. Phase distribution of the link operator.

In 1-d principal chiral models the large- $N$  third order phase transition is consequence of a compactification of the eigenvalues of the link operator

$$L = U(x)U^\dagger(x + \mu) , \quad (12)$$

which are of the form  $\lambda = e^{i\theta}$ . In the weak coupling region ( $\beta > \beta_c$ ) the phase distribution of the eigenvalues of the link operator  $L$ ,  $\rho(\beta, \theta)$  with  $\theta \in (-\pi, \pi]$ , is nonvanishing only in the region  $|\theta| \leq \theta_c(\beta) < \pi$ . The third order critical point  $\beta_c$  is determined by the limit condition  $\theta_c(\beta) = \pi$ , separating the weak coupling from the strong coupling region where  $\rho(\beta, \pi) > 0$  [5].

In order to see if a similar phenomenon characterizes the large- $N$  phase transition also in 2-d, we have extracted from our simulations the phase distribution  $\rho(\beta, \theta)$  of the eigenvalues of  $L$ . Notice that  $\rho(\beta, \theta) = \rho(\beta, -\theta)$  by symmetry, therefore in the following we will show  $\rho(\beta, \theta)$  only in the range  $0 \leq \theta \leq \pi$ . Large- $N$  numerical results seems to support the compactification of the phase distribution at  $\beta_c$ , indeed we found  $\rho(\beta, \pi) \simeq 0$  for  $\beta \gtrsim \beta_{peak}$  ( $\rho(\beta, \pi)$  can be strictly zero only for  $N = \infty$ ). This fact is illustrated in Fig. 6, where we

compare the distributions  $\rho(\beta, \theta)$  at  $\beta = 0.300$  and  $\beta = 0.305$  for  $N = 21$ , whose  $\beta_{peak} \simeq 0.3025$ : the distribution values at  $\theta = \pi$  ( $\rho(0.300, \pi) \simeq 0.010$  and  $\rho(0.305, \pi) \simeq 0.0007$ ) decrease by about a factor 15, becoming very small. Similar behaviors are observed at the other values of  $N$ .

In the  $SU(N)$  models  $\rho(\beta, \theta)$  presents  $N$  maxima, as Fig. 6 shows. This structure is absent in the  $U(N)$  models and should disappear in the large- $N$  limit, in that the height of the peaks with respect to the background curve should vanish. For example, the  $U(N)$  and  $SU(N)$  phase distributions at  $\beta = 0$  are respectively

$$\rho(0, \theta) = \frac{1}{2\pi}, \quad (13)$$

and

$$\rho(0, \theta) = \frac{1}{2\pi} \left[ 1 + (-1)^{N+1} \frac{2}{N} \cos(N\theta) \right]. \quad (14)$$

In our  $SU(N)$  simulations we found the peak heights to decrease approximately as  $1/N$ .

It is also interesting to see how the distributions  $\rho(n, \beta, \theta)$  of the generalized link operators

$$L(n) = U(x)U^\dagger(x + n\mu), \quad (15)$$

( $\rho(1, \beta, \theta) \equiv \rho(\beta, \theta)$ ) evolve as function of the distance  $n$ . In Fig. 7 we plot  $\rho(n, \beta, \theta)$  for  $N = 15$ , at  $\beta = 0.305$  ( $\xi_G \simeq 3.79$ ) and for various values of  $n$ . When  $d \equiv n/\xi \rightarrow \infty$ ,  $\rho(n, \beta, \theta)$  appears to tend to the  $\beta = 0$  distribution (14).

#### D. Critical slowing down around the large- $N$ singularity.

The large- $N$  critical behavior causes a phenomenon of critical slowing down in the Monte Carlo simulations. At sufficiently large  $N$  ( $N \gtrsim 15$ ) and for both  $U(N)$  and  $SU(N)$  models, the autocorrelation times of the internal energy  $\tau_E$  and the magnetical susceptibility  $\tau_\chi$  (estimated by a blocking procedure) showed a maximum around the peak of the specific heat, and a sharper and sharper behavior with growing  $N$ . The increase of the autocorrelation times, with growing  $N$ , was much larger around the specific heat peak than elsewhere. In the  $SU(N)$  simulations,  $\tau_E$  ( $\tau_\chi$ ) went from  $\sim 600$  ( $400$ ) at  $\beta = 0.3025$  and  $N = 21$  to  $\sim 3000$  ( $2500$ ) at  $\beta = 0.304$  and  $N = 30$  (the uncertainty on this numbers is large, they are just indicative). After the peak of  $C$   $\tau_E$  and  $\tau_\chi$  decreased, for example at  $N = 30$  and  $\beta = 0.305$   $\tau_E \simeq 700$  and  $\tau_\chi \simeq 300$ . Similar behavior was observed in the  $U(N)$  simulations. The above critical slowing down phenomenon represents the most serious difficulty in getting numerical results around  $\beta_c$  at larger  $N$  by the Monte Carlo algorithm used in this work. At large correlation length  $\tau_\chi$  increases again due the critical slowing down associated to the continuum limit, while  $\tau_E$  tends to be stable.

We want to mention an attempt for a better algorithm in the  $U(N)$  case, by constructing a microcanonical updating involving globally the  $U(N)$  matrix instead of using its subgroups. A microcanonical updating of  $U$  according to the action

$$A(U) = \text{Re Tr} [UF] \quad (16)$$

can be achieved by performing the reflection with respect to the  $U(N)$  matrix  $U_{max}$  which maximizes  $A(U)$ :

$$\begin{aligned} U_{new} &= U_{max} U_{old}^\dagger U_{max} , \\ U_{max} &= \frac{1}{\sqrt{F^\dagger F}} F^\dagger . \end{aligned} \quad (17)$$

Notice that the determination of  $U_{max}$  requires the diagonalization of the complex matrix  $F$ . The update (17) does not change the action and it must be combined with ergodic algorithms (e.g. heat bath). We found that, at large  $N$  and in the region of  $\beta$  values we considered, the algorithm based on the  $SU(2)$  and  $U(1)$  subgroups performs better than those based on the updating (17). The latter may become convenient at relatively small  $N$  and/or for larger correlation lengths. On the other hand, at large space correlation lengths multigrid algorithms should eventually become more efficient, in that they should have smaller dynamical exponents (see Refs. [19,20] for some implementations of multigrid algorithms in the context of lattice chiral models).

## APPENDIX A

The free energy of 1-d  $U(N)$  lattice chiral models can be written in terms of a determinant of modified Bessel functions

$$F(N, \beta) = \frac{1}{N^2} \ln Z(N, \beta) = \frac{1}{N^2} \ln \det I_{j-i}(2N\beta) . \quad (A1)$$

The specific heat can be obtained by

$$C(N, \beta) = \frac{1}{N} \frac{dE}{dT} = \frac{1}{2} \beta^2 \frac{d^2 F}{d\beta^2} . \quad (A2)$$

The large- $N$  limit of the specific heat shows the existence of a third order phase transition at  $\beta_c = 1/2$ , indeed we have

$$\begin{aligned} C(\infty, \beta) &= \beta^2 & \text{for } \beta \leq \beta_c , \\ C(\infty, \beta) &= \frac{1}{4} & \text{for } \beta \geq \beta_c . \end{aligned} \quad (A3)$$

The singularity at  $\beta_c$  can be characterized by a critical exponent  $\alpha = -1$ . From the double scaling limit of the corresponding unitary matrix model the correlation length exponent turns out to be  $\nu = 3/2$  [21].  $\alpha$  and  $\nu$  satisfy a hyperscaling relationship associated to a two-dimensional critical phenomenon:  $2\nu = 2 - \alpha$ .

1-d  $U(N)$  lattice chiral models present a peak in the specific heat, whose position  $\beta_{peak}(N)$  should approach  $\beta_c$  with increasing  $N$ . The finite  $N$  scaling arguments already mentioned in this paper lead to the Ansatz (10) for the positions of the specific heat peaks. In Table III we report the values of  $\beta_{peak}(N)$  and  $C(N, \beta_{peak})$  as function of  $N$  up to  $N = 11$ . As shown in Fig. 8, the large  $N$  behavior of  $\beta_{peak}(N)$  is well fitted by

$$\beta_{peak}(N) = \beta_c + aN^{-\epsilon} + bN^{-2\epsilon} \quad (A4)$$

with  $\epsilon = 2/3$ , and therefore  $\nu = 1/\epsilon = 3/2$  ( $a \simeq 0.595$  and  $b \simeq 0.13$ ). The result  $\nu = 3/2$  was also found in the finite  $N$  scaling of the partition function zeroes [7].



## REFERENCES

- [1] F. Green and S. Samuel, Nucl. Phys. **B190**, 113 (1981).
- [2] M. Campostrini, P. Rossi and E. Vicari, “Asymptotic scaling from strong coupling”, IFUP-TH 36/94 (1994).
- [3] M. Campostrini, P. Rossi and E. Vicari, “Strong coupling expansion of chiral models”, IFUP-TH 63/94 (1994); “Strong coupling analysis of 2-d large-N lattice chiral models”, IFUP-TH 64/94 (1994).
- [4] P. Rossi and E. Vicari, Phys. Rev. **D 49** (1994) 6072; **D 50** (1994) 4718 (E).
- [5] D. J. Gross and E. Witten, Phys. Rev. **D 21**, 446 (1980).
- [6] E. Brezin and J. Zinn-Justin, Phys. Lett. **288B**, 54 (1992).
- [7] P. H. Damgaard and U. M. Heller, Nucl. Phys. **B410**, 494 (1993).
- [8] F. Green and S. Samuel, Phys. Lett. **103B**, 110 (1981).
- [9] R. Gupta and C. Baillie, Phys. Rev. **D 45**, 2883 (1992).
- [10] N. Cabibbo and E. Marinari, Phys. Lett. **119B**, 387 (1982).
- [11] R. Petronzio and E. Vicari, Phys. Lett. **254B**, 444 (1991).
- [12] J. W. Carlson, Nucl. Phys. **B248**, 536 (1984).
- [13] A. M. Ferrenberg and R. H. Swendsen, Phys. Rev. Lett. **61** (1988) 2635; Phys. Rev. Lett. **63** (1989) 1196.
- [14] E. Brezin and V. Kazakov, Phys. Lett. **236B**, 144 (1990).
- [15] D. Gross and A. Migdal, Phys. Rev. Lett. **64** (1990) 127.
- [16] H.E. Stanley, Introduction to phase transitions and critical phenomena, Clarendon Press, Oxford, 1971.
- [17] G. Parisi, in High Energy Physics 1980, Proceedings of the XXth Conference on High Energy Physics, Madison, Wisconsin, 1980, edited by L. Durand and L. G. Pondrom, AIP Conf. Proc. No. 68 (AIP, New York, 1981).
- [18] F. Green and S. Samuel, Nucl. Phys. **B194**, 107 (1982).
- [19] R. G. Edwards, S. J. Ferreira, J. Goodman and A. D. Sokal, Nucl. Phys. **B380**, 621 (1992).
- [20] M. Hasenbusch and S. Meyer, Phys. Rev. Lett. **68** (1992) 435.
- [21] V. Periwal and D. Shevitz, Phys. Rev. Lett. **64** (1990) 1326.

## FIGURES

FIG. 1. Specific heat vs.  $\beta$  for  $SU(N)$  models. The solid line represents the strong-coupling determination, whose estimate of the critical  $\beta$  is indicated by the vertical dashed lines. The thick solid lines above the peaks represent our estimates of  $\beta_{peak}$ .

FIG. 2. Specific heat vs.  $\beta$  for  $U(N)$  models. The solid line represents the strong-coupling determination, whose estimate of the critical  $\beta$  is indicated by the vertical dashed lines. The large solid lines above the peaks represent our estimates of  $\beta_{peak}$ .

FIG. 3.  $\beta_{peak}(N)$  vs.  $1/N$ . The dashed lines show the fit result.

FIG. 4.  $\xi_G$  vs.  $\beta$ . The solid line represents the strong-coupling determination, whose estimate of the critical  $\beta$  is indicated by the vertical dashed lines.

FIG. 5.  $\chi_d$  vs.  $\beta$ . The vertical dashed line indicates the estimate of  $\beta_c$ . The filled symbols indicate the positions of the peak of  $C$  at  $N = 9, 15, 21$ .

FIG. 6.  $\rho(\beta, \theta)$  for the  $SU(21)$  model at  $\beta = 0.300$  and  $\beta = 0.305$ .

FIG. 7.  $\rho(n, \beta, \theta)$  for the  $SU(15)$  model at  $\beta = 0.305$  for various value of  $n$ .

FIG. 8.  $\beta_{peak}(N)$  vs.  $1/N$  in 1-d  $U(N)$  lattice chiral models.

TABLES

TABLE I. Numerical results for  $U(N)$ .

$N$	$\beta$	$L$	Stat	$E$	$C$	$\chi$	$\xi_G$	$\chi_d$	$\xi_d$
9	0.30	24	100k	0.60374(8)	0.284(6)	10.50(3)	2.058(14)	1.64(2)	0.6(2)
	0.31	30	150k	0.56706(9)	0.427(11)	15.43(4)	2.649(17)	2.82(4)	1.0(2)
	0.313	30	300k	0.55215(10)	0.541(11)	18.53(5)	2.972(14)	3.93(5)	1.2(2)
	0.315	36	150k	0.54077(14)	0.61(2)	21.80(10)	3.36(3)	5.59(9)	1.9(2)
	0.318	36	300k	0.52128(10)	0.66(2)	29.47(9)	4.08(3)	11.3(2)	3.0(2)
	0.3185	36	400k	0.51799(11)	0.69(2)	31.17(11)	4.22(2)	12.8(2)	3.2(2)
	0.319	42	300k	0.51482(11)	0.69(2)	32.86(13)	4.38(3)	14.7(4)	3.3(3)
	0.320	42	400k	0.50816(10)	0.66(2)	37.2(2)	4.73(3)	20.5(5)	4.3(3)
	0.323	48	330k	0.49172(9)	0.50(2)	51.6(3)	5.83(4)	55(3)	8.5(5)
	0.323	60	200k	0.49166(11)	0.52(2)	51.7(3)	5.79(7)	57(3)	7.7(7)
15	0.28	18	150k	0.65373(4)	0.163(3)	6.924(7)	1.519(4)	1.030(8)	
	0.30	24	200k	0.60276(6)	0.300(10)	10.81(2)	2.063(9)	1.29(2)	
	0.305	24	180k	0.58405(9)	0.396(12)	13.09(3)	2.346(9)	1.57(2)	
	0.308	30	250k	0.56875(9)	0.57(2)	15.55(3)	2.632(10)	2.14(2)	0.7(2)
	0.310	30	300k	0.55423(12)	0.78(3)	18.83(5)	2.996(11)	3.31(5)	1.2(2)
	0.311	30	500k	0.54453(10)	0.97(4)	21.58(4)	3.276(8)	4.87(6)	1.6(1)
	0.311	36	300k	0.54470(13)	0.97(4)	21.52(6)	3.276(14)	4.85(9)	1.5(2)
	0.312	36	600k	0.53374(11)	1.05(4)	25.57(10)	3.67(2)	8.42(15)	2.8(2)
	0.313	36	500k	0.52365(12)	0.94(4)	30.42(10)	4.131(15)	14.5(5)	3.7(3)
	0.315	42	200k	0.50920(10)	0.50(3)	40.0(2)	4.95(4)	42(5)	7.2(7)
0.315	48	300k	0.50915(7)	0.49(2)	39.7(2)	4.89(4)	46(3)	8.1(7)	
21	0.28	18	100k	0.65373(4)	0.162(4)	6.972(8)	1.526(5)	0.991(8)	
	0.30	24	200k	0.60273(6)	0.303(9)	10.881(13)	2.069(6)	1.140(8)	
	0.3025	24	300k	0.59390(6)	0.361(10)	11.869(14)	2.185(6)	1.220(9)	
	0.305	30	300k	0.58318(6)	0.446(14)	13.31(2)	2.364(9)	1.394(11)	
	0.308	30	200k	0.56337(15)	0.88(6)	16.79(5)	2.748(13)	2.15(3)	
	0.309	30	300k	0.5512(3)	1.31(13)	19.92(10)	3.09(2)	3.60(9)	1.2(2)
	0.3095	30	450k	0.5415(3)	1.98(15)	23.11(13)	3.43(2)	6.6(3)	2.4(2)
	0.31	36	300k	0.5337(2)	1.28(10)	26.23(11)	3.75(2)	11.1(5)	3.4(3)

TABLE II. Numerical results for  $SU(N)$ . When more than one lattice size appears, the corresponding results were obtained collecting data of simulations at the reported lattice sizes (which were, in all cases, in agreement within the errors).

$N$	$\beta$	$L$	Stat	$E$	$C$	$\chi$	$\xi_G$
9	0.290	30	200k	0.58774(8)	0.412(7)	13.32(3)	2.353(11)
	0.294	30,36	600k	0.56788(6)	0.435(6)	16.89(3)	2.793(14)
	0.295	24,30,36,42	900k	0.56284(4)	0.443(5)	18.00(2)	2.910(9)
	0.2955	36	500k	0.56026(5)	0.442(6)	18.58(4)	2.95(2)
	0.296	30,36	600k	0.55781(5)	0.438(6)	19.20(3)	3.03(2)
	0.2965	36	600k	0.55531(6)	0.436(6)	19.86(4)	3.08(2)
	0.300	30,36,42	350k	0.53846(9)	0.413(11)	25.27(7)	3.66(2)
	0.310	42,48,54	500k	0.50030(4)	0.306(5)	47.25(12)	5.43(3)
15	0.295	24	200k	0.60013(11)	0.47(2)	11.47(2)	2.149(9)
	0.299	30	300k	0.57564(10)	0.66(2)	15.07(3)	2.577(11)
	0.300	24	400k	0.56798(10)	0.69(4)	16.55(3)	2.738(6)
	0.300	30	400k	0.56805(10)	0.70(3)	16.57(3)	2.746(9)
	0.300	36	600k	0.56807(9)	0.66(2)	16.58(2)	2.745(8)
	0.300	42	500k	0.56810(5)	0.70(2)	16.57(3)	2.752(12)
	0.3005	36	600k	0.56430(7)	0.68(2)	17.41(3)	2.833(11)
	0.301	36	500k	0.56054(6)	0.68(2)	18.31(3)	2.940(10)
	0.302	36	500k	0.55300(5)	0.65(2)	20.26(3)	3.131(9)
	0.305	36	500k	0.53418(6)	0.516(13)	26.86(6)	3.786(11)
	0.310	45	300k	0.51178(4)	0.354(7)	39.06(10)	4.80(2)
21	0.300	24	300k	0.58810(10)	0.65(3)	12.90(2)	2.310(6)
	0.302	30	500k	0.57049(13)	1.00(4)	15.91(3)	2.665(7)
	0.302	36	600k	0.57069(8)	0.95(3)	15.87(2)	2.659(8)
	0.3025	24	400k	0.56490(20)	1.14(6)	17.09(6)	2.787(8)
	0.3025	30	400k	0.56517(14)	1.02(5)	17.02(4)	2.784(8)
	0.3025	36	500k	0.56491(11)	1.04(5)	17.11(4)	2.800(10)
	0.303	36	500k	0.55959(9)	0.96(4)	18.38(3)	2.936(9)
	0.305	30	500k	0.54100(8)	0.72(2)	24.14(5)	3.526(8)
	0.310	42	240k	0.51548(6)	0.41(2)	36.66(12)	4.61(2)
30	0.300	24	150k	0.59927(8)	0.38(2)	11.35(2)	2.114(7)
	0.3025	30	200k	0.58479(10)	0.79(5)	13.24(3)	2.338(7)
	0.303	30	200k	0.58007(15)	1.00(8)	13.99(4)	2.433(10)
	0.304	24	500k	0.5625(4)	2.4(3)	17.55(7)	2.857(10)
	0.304	30	500k	0.5632(3)	2.3(2)	17.40(7)	2.829(8)
	0.305	30	200k	0.5466(2)	1.05(10)	22.13(5)	3.320(12)

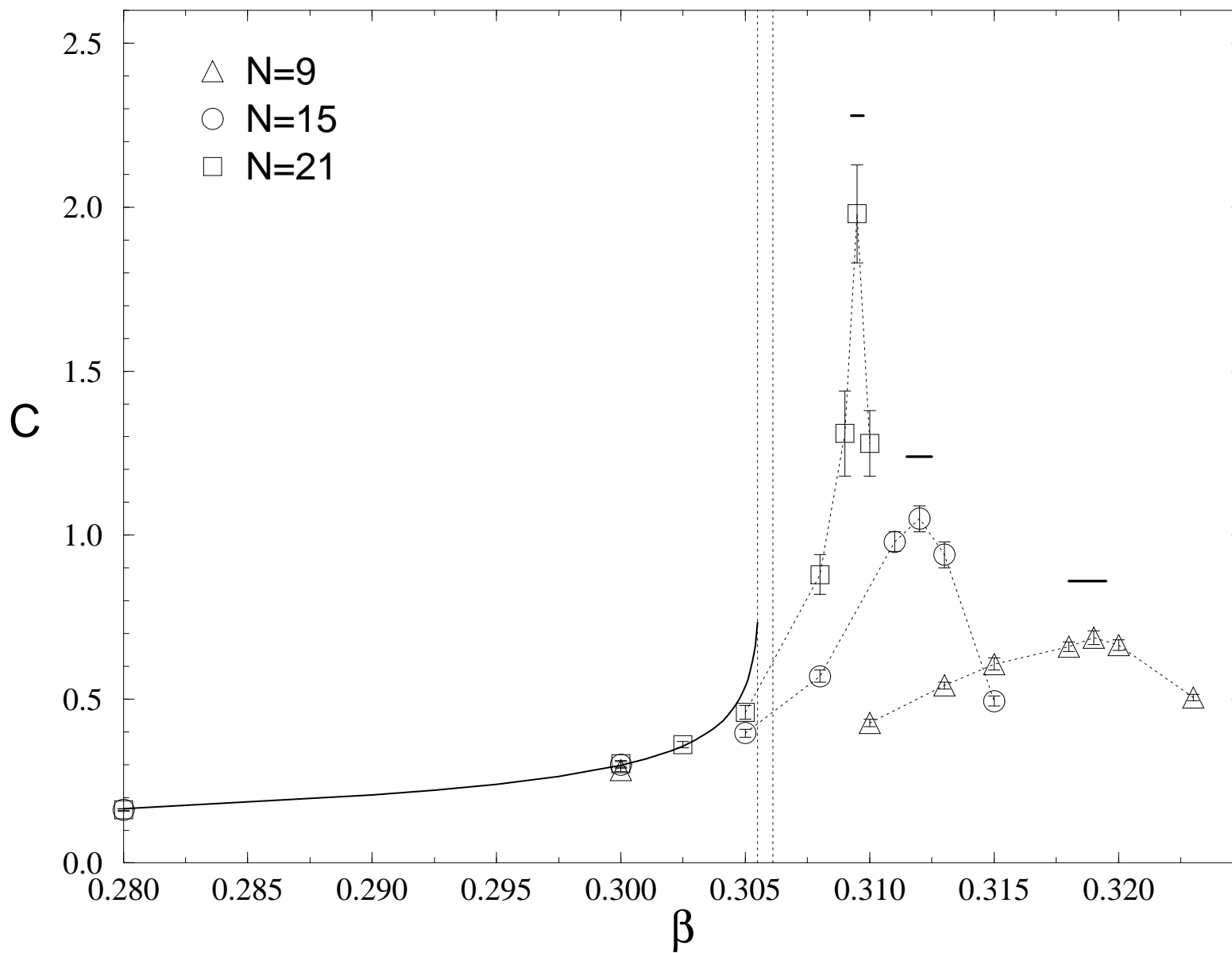
TABLE III.  $\beta_{peak}(N)$  and  $C(N, \beta_{peak})$  versus  $N$  for 1-d  $U(N)$  lattice chiral models.

$N$	$\beta_{peak}$	$C(\beta_{peak})$
2	0.930889	0.29461215
3	0.818356	0.27992604
4	0.758001	0.27269388
5	0.719664	0.26839003
6	0.692846	0.26553250
7	0.672876	0.26349442
8	0.657337	0.26196545
9	0.644848	0.26077452
10	0.634554	0.25981956
11	0.625899	0.25903594

This figure "fig1-1.png" is available in "png" format from:

<http://arxiv.org/ps/hep-lat/9412102v1>

Figure 1



This figure "fig2-1.png" is available in "png" format from:

<http://arxiv.org/ps/hep-lat/9412102v1>

This figure "fig3-1.png" is available in "png" format from:

<http://arxiv.org/ps/hep-lat/9412102v1>



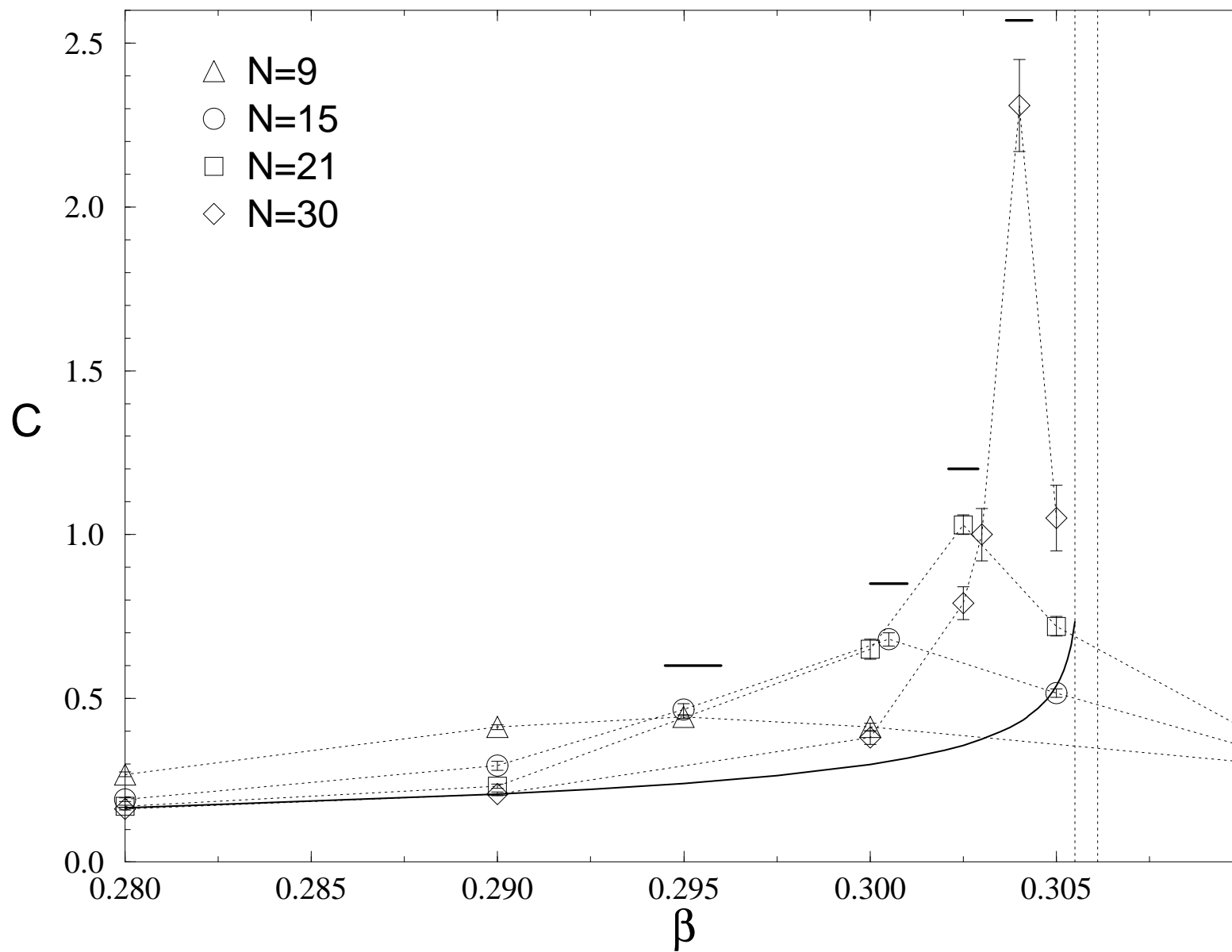
This figure "fig1-2.png" is available in "png" format from:

<http://arxiv.org/ps/hep-lat/9412102v1>

This figure "fig2-2.png" is available in "png" format from:

<http://arxiv.org/ps/hep-lat/9412102v1>

Figure 2



This figure "fig3-2.png" is available in "png" format from:

<http://arxiv.org/ps/hep-lat/9412102v1>

This figure "fig1-3.png" is available in "png" format from:

<http://arxiv.org/ps/hep-lat/9412102v1>

This figure "fig2-3.png" is available in "png" format from:

<http://arxiv.org/ps/hep-lat/9412102v1>

Figure 3

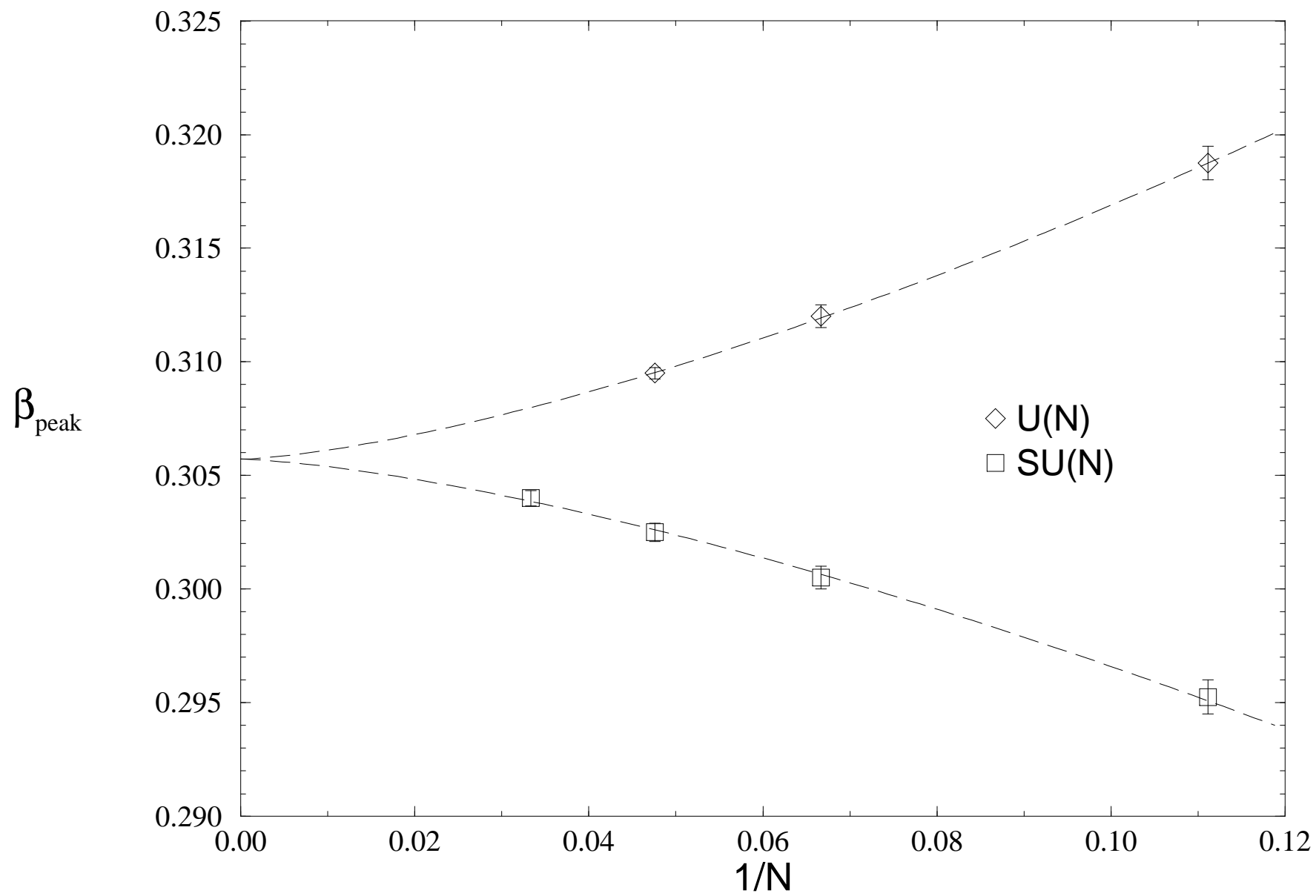


Figure 4

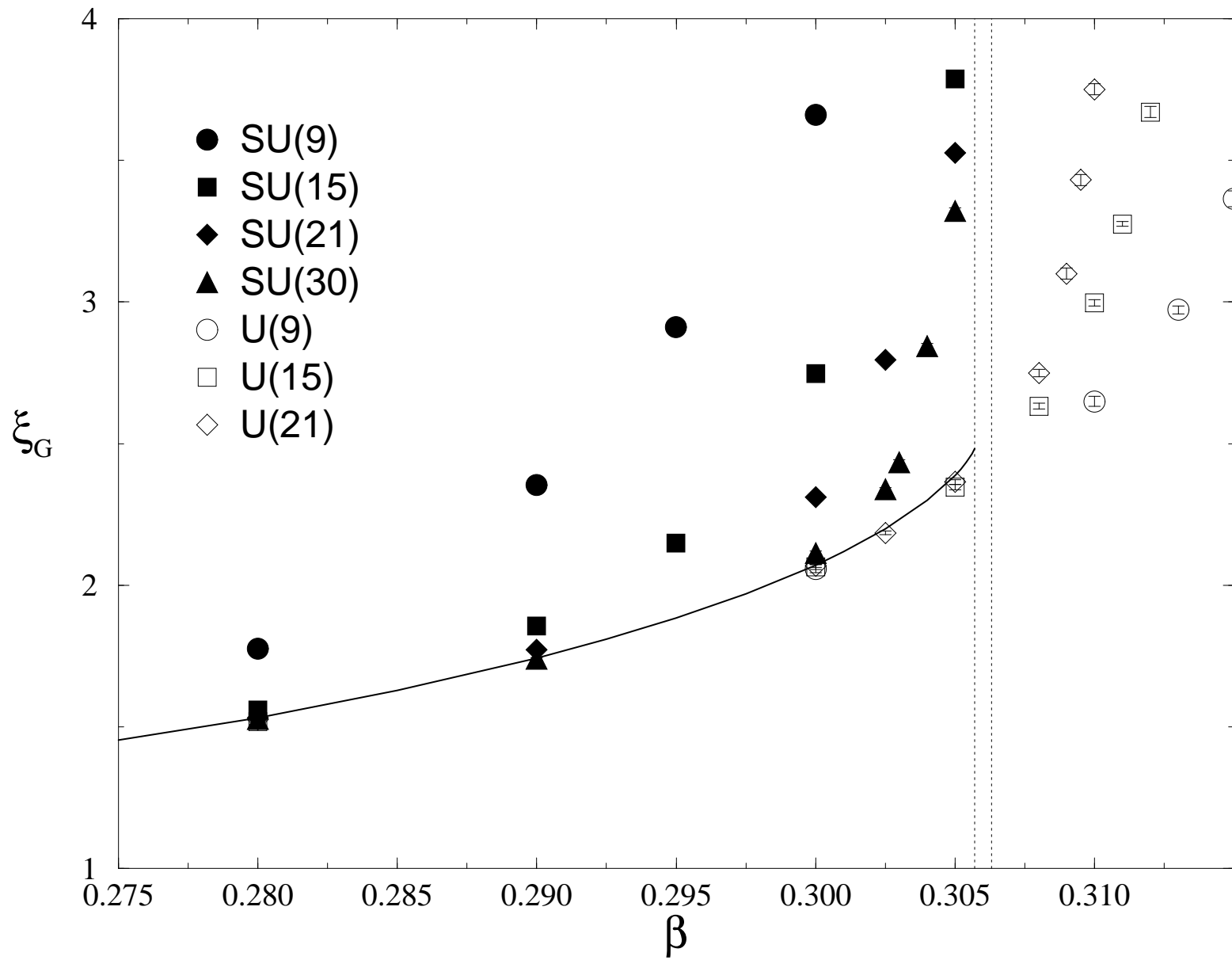




Figure 5

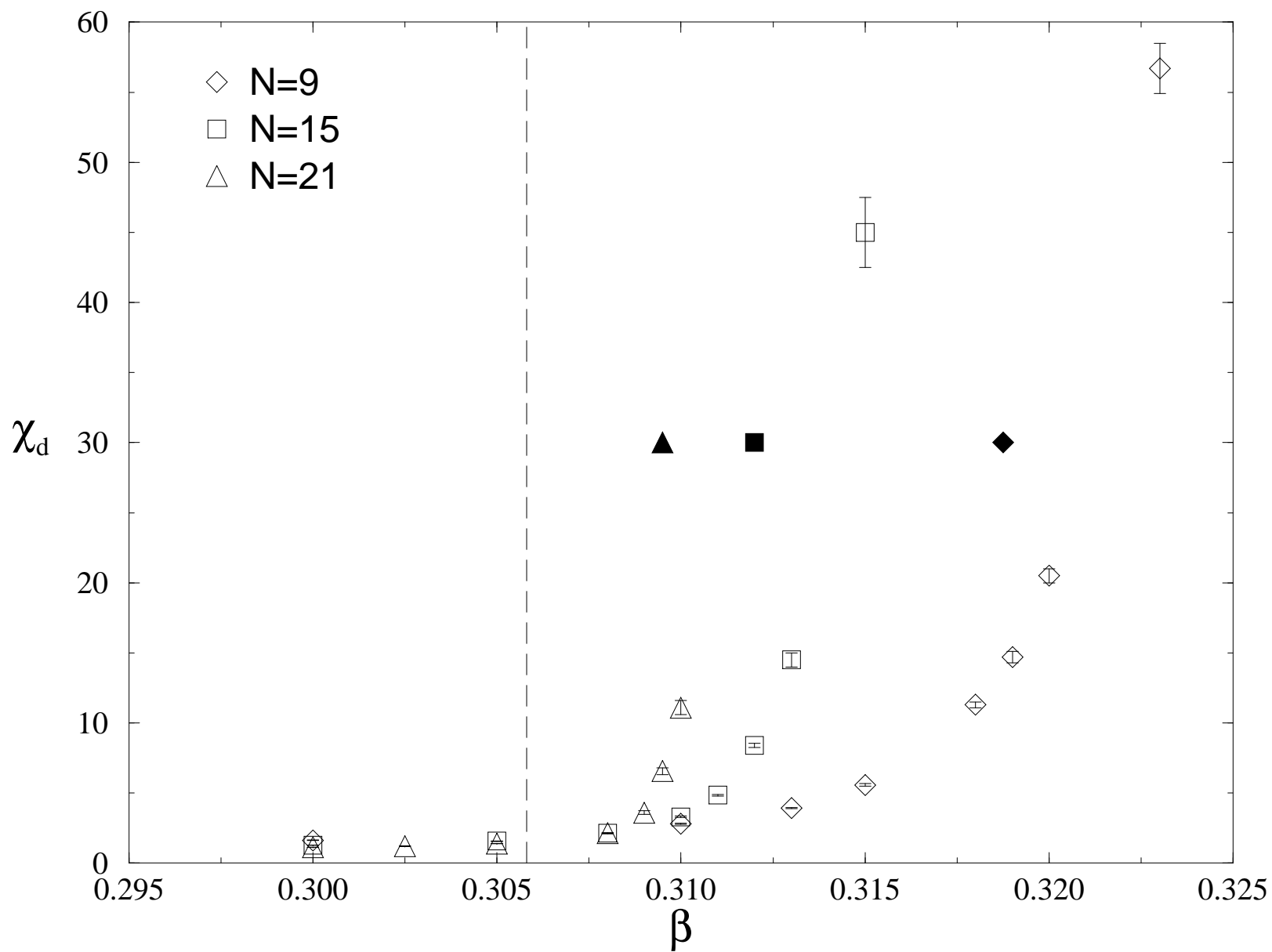


Figure 6

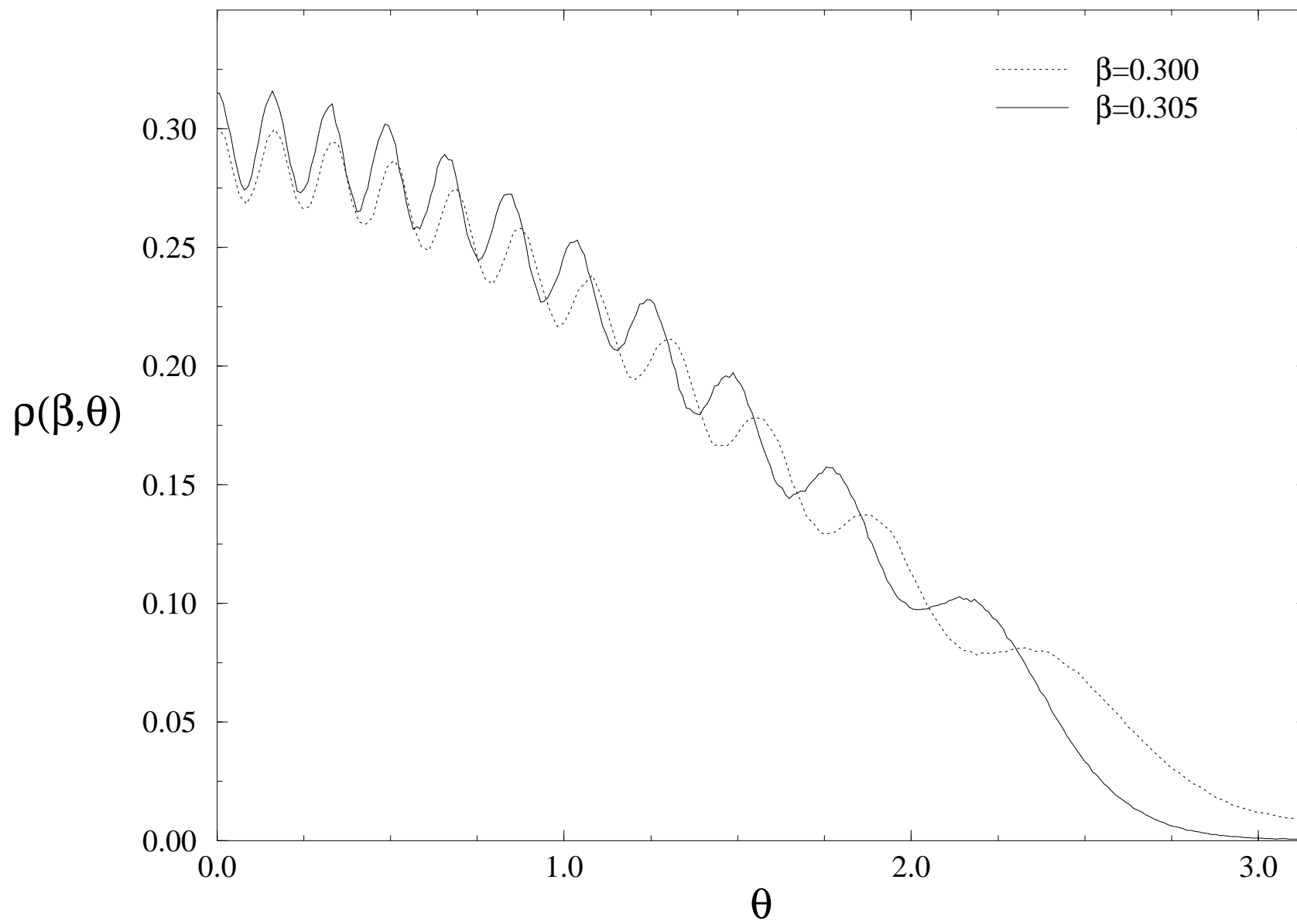


Figure 7

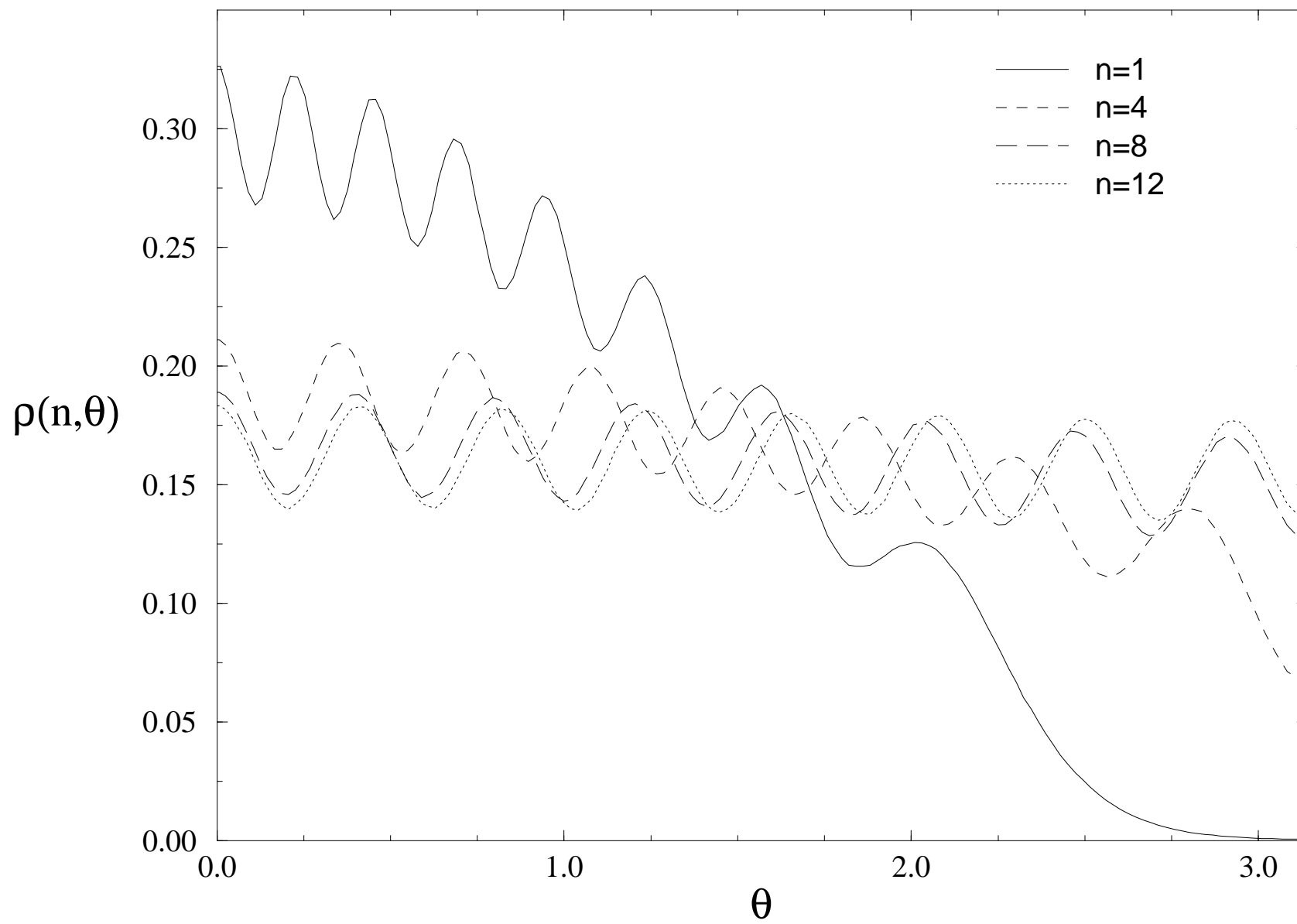


Figure 8

